

Calculation of Gas and Electronic Temperatures in the Channel of the Direct Current Arc

Alexander V. Gerasimov · Alexander P. Kirpichnikov

Published online: 5 August 2009
© Springer Science+Business Media, LLC 2009

Abstract The results of calculations of gas and electronic temperatures in the channel of an arc plasma generator are presented. The calculations were carried out within the framework of a self-consistent two-temperature channel model of an arc discharge. The given method can be used with good precision to determine the radial distribution of gas and electronic temperatures in conducting and non-conducting zones of a constant current arc at designated parameters of the discharge (current intensity and power).

Keywords Arc · Channel · Discharge · Model · Plasma · Temperature

1 Introduction

Numerical modeling of gas heating processes in a channel of arc plasmatron is a very laborious task. The wish to create a mathematical model of the aforementioned processes generates a need of a numerical solution of the magnetic hydrodynamic equations. The solution of these equations has many additional problems concerning the nonlinearity of the system, the choice of differential equation scheme, the boundary conditions etc.

Unfortunately, universal procedures to solve these problems do not exist. Successful approaches can be sought which adequately describe the physical processes with minimal mathematical cost in terms of model simplicity and its implementation. The importance of such investigations is evident, because they offer a guide to optimal device operation selection for power engineering specialists.

A. V. Gerasimov (✉) · A. P. Kirpichnikov
Kazan State Technology University, Kazan 420015, Russian Federation
e-mail: gerasimov@kstu.ru

In some cases, the description of physical processes in an electrical arc permits an analytical solution with advantages over numerical solutions. The formula and algorithm construction for calculating the field parameters with a minimal quantity of experimental data and their computer implementation must be considered.

In our previous study [1], we considered the quasi-equilibrium channel model of a direct current arc on the assumption that electron and heavy-particle temperatures near the axis do not severely differ from each other.

However, such a simplification is not always valid. It is known that even under atmospheric pressure the near-arc-axis discharge can exhibit considerably different temperatures of atomic–ionic gas and electron temperatures, the value of which in practice can be rather large (several hundred degrees). It has been established in the literature that this case occurs in arcs at atmospheric pressure with discharge currents $I \leq 50$ A [2]. This article presents a dual temperature channel arc model based on results obtained earlier [1]. The model takes into account the difference between the temperature of the atomic–ionic gas of heavy particles and the electronic temperature in the discharge region.

2 Theoretical Part

It is necessary to introduce an arc channel model characterized by discharge plasma equilibrium. We consider a long cylindrical column of the arc in a longitudinal cylindrical field. The arc burns inside a cooled tube of a radius R . Heat is released to the walls by a radial thermal stream with the temperature assumed to be fixed and low. The radial temperature distribution is shown in Fig. 1. There is a well-defined area near the axis (its radius marked as r_0) inside which current flow is almost entirely confined. Approximately, at $r > r_0$, $\sigma = 0$, and at $r < r_0$, $\sigma = \text{const} = \sigma_c$, where σ is the electronic conductivity and σ_c is the channel conductivity corresponding to maximum plasma temperature on the T_c axis: $\sigma_c = \sigma(T_c)$. The boundary line between the conducting and non-conducting zones is located at the position where the conductivity drops to the $1/e$ of the maximum value $\sigma_c = \sigma(T_c)$ (see Fig. 1) [3,4].

According to experiment and theory, at $T = 5,000$ K, the value of $\sigma(T) \approx 2 \Omega^{-1} \cdot \text{cm}^{-1}$; at $T = 10,000$ K, the value is $\sigma(T) \approx 38 \Omega^{-1} \cdot \text{cm}^{-1}$; at $T = 12,000$ K the value is $\sigma(T) \approx 40 \Omega^{-1} \cdot \text{cm}^{-1}$; at $T = 14,000$ K, the value is $\sigma(T) \approx 41 \Omega^{-1} \cdot \text{cm}^{-1}$, etc. Therefore, in this case, the boundary conditions of the current-conducting channel correspond to a temperature of about 10,000 K [5,6].

It is well known that the solution of the heat balance equation for a non-conducting zone is [4]

$$T_g(r) = T_g(R) + \frac{W}{2\pi\lambda} \ln \frac{R}{r} \quad (1)$$

and matches the experimental values [3] for high-current arcs with current $I > 200$ A. In Eq. 1, T_g is a gas temperature, W is the power injected into one unit of the column length, λ is the gas thermal conductivity, and R is the tube radius.

In [1], the authors obtained temperature fields in the non-conducting zone of discharge that are described by the following formulas:

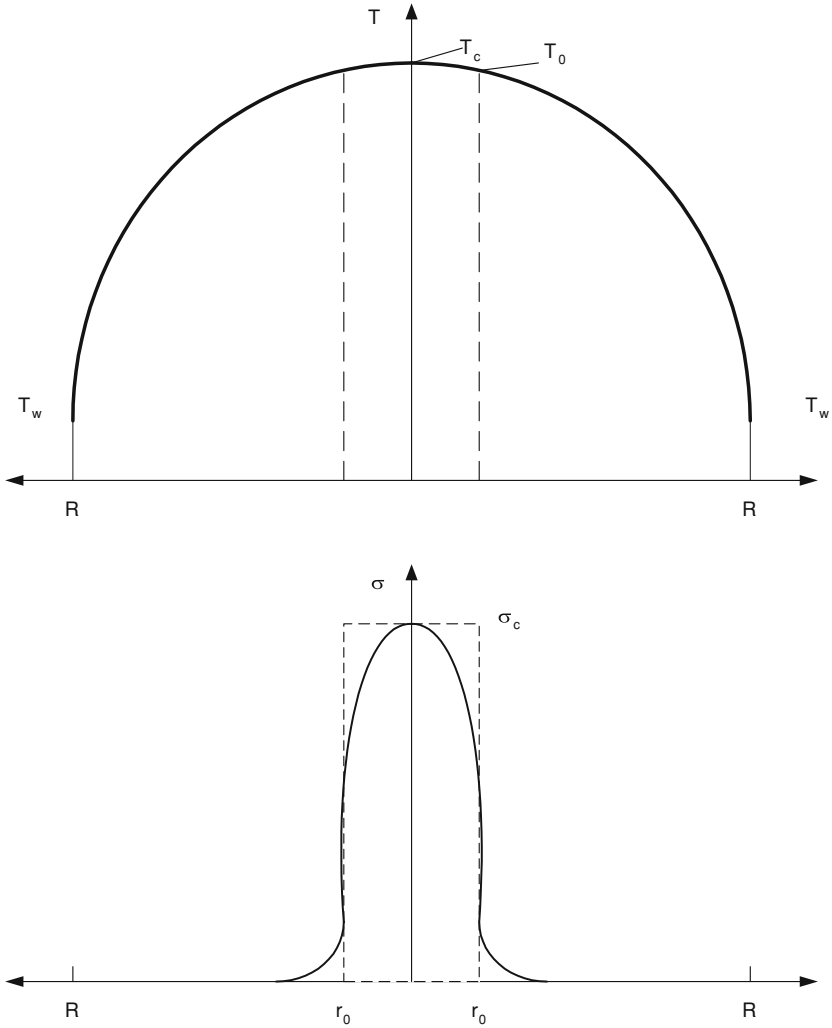


Fig. 1 Schematic distributions of temperature and conductivity on radius in the arc discharge by channel model

$$T_e(r) = T_e(R) + \frac{W}{2\pi\lambda} \ln \frac{R}{r} + \left(\frac{W}{2\pi\lambda} + \varepsilon R \right) \frac{\lambda_e \Psi(R) + \lambda_{ai} \Psi(r)}{\lambda_{ai} b R \Phi(r_c)} \quad (2)$$

$$T(r) = T(R) + \frac{W}{2\pi\lambda} \ln \frac{R}{r} + \left(\frac{W}{2\pi\lambda} + \varepsilon R \right) \frac{\lambda_e [\Psi(R) - \Psi(r)]}{\lambda_{ai} b R \Phi(r_c)} \quad (3)$$

where T_e is the electronic gas temperature; T is the temperature of heavy-particle atomic–ionic gas; λ_e is the electronic gas thermal conductivity coefficient; λ_{ai} is the atomic–ionic gas thermal conductivity coefficient; $I_{0,1}(x)$ and $K_{0,1}(x)$ are modified Bessel functions of the first and second kind of order zero and one, respectively; $\lambda = \lambda_{ai} + \lambda_e$; and r_c is the radius of the channel [3]. The following functions have also been defined:

$$\Phi(r_c) = K_0(br_c)I_1(bR) + I_0(br_c)K_1(bR), \tag{4}$$

$$\Psi(r) = K_0(br_c)I_0(br) - I_0(br_c)K_0(br). \tag{5}$$

$$r_c \leq r \leq R.$$

From [1], it follows that in the conducting zone $T_e = T$.

These expressions take into account the temperature difference between electronic and atomic–ionic gases in the non-conducting zone of discharge and describe well the temperature fields in discharges in the current range of 50 A to 200 A. However, in the case $I \leq 50$ A, it is also necessary to take into account the temperature difference between electronic and atomic–ionic gases in the conducting area of the arc discharge.

As in [1], we assume that $T_{e0} \equiv T_e(r_c) \approx T_e(0) \equiv T_{ec}$, where r_c is the channel radius, defined according to [3]. In this case, the correlation between the temperature on channel axis T_{ec} , and the power introduced per unit length of the discharge column, W , may be written as follows:

$$T_{ec} = \sqrt{\frac{TW}{8\pi\lambda_e k} - \frac{T_c - T_0}{2k} \frac{\lambda_{ai}}{\lambda_e} I_i} \tag{6}$$

In this formula, $T_c \equiv T(0)$ and $T_0 \equiv T(r_c)$ are gas temperatures on the channel axis and boundary, respectively; $\lambda_e = \lambda_e(T_c)$ and $\lambda_{ai} = \lambda_{ai}(T_c)$ are the thermal conductivities for electronic and atomic–ionic gases, respectively; I_i is the ionization potential of the plasma forming gas; and k is Boltzmann’s constant. As for the discharge conductivity, it is directly proportional to the electron concentration and is given by $\sigma \sim n_e \approx \text{const} \cdot e^{-\frac{I_i}{2kT_{ec}}}$ [2].

The main goals of this article are to express $T_c = T_c(T_{ec})$ and $T_0 = T_0(T_{ec})$ as functions of T_{ec} , and then to obtain T_{ec} and r_c at a given power, W [3,4].

A system of equations for energy balance in the arc, which considers dissipation in the form of radiation, was obtained in [1].

In the current-conducting channel, $T_e \approx \text{const} = T_{ec}$ and

$$\frac{1}{r} \frac{\partial}{\partial r} \left(r\lambda_{ai} \frac{\partial T}{\partial r} \right) + \frac{3}{2} k\delta n_e \nu (T_{ec} - T) = 0 \tag{7}$$

and in the non-conducting (heat removal) zone,

$$\frac{1}{r} \frac{\partial}{\partial r} \left(r\lambda_e \frac{\partial T_e}{\partial r} \right) - \frac{3}{2} k\delta n_e \nu (T_e - T) = 0 \tag{8}$$

$$\frac{1}{r} \frac{\partial}{\partial r} \left(r\lambda_{ai} \frac{\partial T}{\partial r} \right) + \frac{3}{2} k\delta n_e \nu (T_e - T) = 0 \tag{9}$$

where n_e is the electron density in the discharge; δ is the energy lost by electrons scattered by heavy particles (collisions); and ν is the collision frequency. Since argon is a monoatomic gas, the constant δ is considered to be close to 1.

Equation 7 expresses the energy balance for the electronic gas; Eqs. 8 and 9 describe that for atoms and ions.

For further calculations using these and subsequent formulas, the coefficients λ_e , λ_{ai} , δ , ν , and n_e will be considered equal to their average values inside the discharge.

However, there is another possible method used for estimating the atomic–ionic temperature in the channel conducting zone [7]:

$$T_{ec} - T = \frac{\sigma E^2}{3/2kn_e\nu}, \tag{10}$$

where

$$\nu = \sqrt{\frac{8 kT_{ec}}{\pi m_e}} (n_e Q_{ei} + n Q_{en}), \tag{11}$$

$$\sigma = \frac{e^2 n_e}{m_e \nu}, \tag{12}$$

where Q is an effective collision cross section, and E is the electric field intensity. This is only an estimate of the atomic temperature and is different from Eq. 7 which allows for the radial distribution of the atomic–ionic temperature inside of the current-conducting canal.

The boundary conditions for system Eqs. 7–9 are [1]

$$\begin{aligned} T(0) < \infty; \quad T(R) = \text{const}; \quad T(r_c - 0) = T(r_c + 0); \\ T_e(r_c - 0) = T_e(r_c + 0); \quad \lambda_e \frac{\partial T_e}{\partial r} \Big|_{r=r_c} + \lambda_{ai} \frac{\partial T}{\partial r} \Big|_{r=r_c} = -\frac{W}{2\pi r_c}; \tag{13} \\ \frac{\partial T_e}{\partial r} \Big|_{r=R} = \varepsilon \quad (\varepsilon \geq 0). \end{aligned}$$

The value of ε depends on discharge parameters, and it is chosen in specific cases according to the physical model used for the interaction between the electronic gas and the walls of the cylindrical pipe [8].

The system of Eqs. 7–9 in agreement with boundary conditions of Eq. 13 has the following exact solution inside of the channel written in terms of the special functions $I_{0,n}(x)$ and $K_{0,n}(x)$:

$$\begin{aligned} T(r) - T_{ec} = \frac{I_0(ar)}{I_0(ar_c)} \left[T(R) - T_{ec} + \frac{W}{2\pi\lambda} \ln \frac{R}{r_c} + \left(\frac{W}{2\pi\lambda} + \varepsilon R \right) \right. \\ \times \frac{I_0(bR) - I_0(br_c)}{\lambda b R I_1(bR)} \frac{\lambda_e}{\lambda_{ai}} - \frac{W}{2\pi\lambda} \ln \frac{R}{r_c} \alpha(r_c) \\ \left. - \left(\frac{W}{2\pi\lambda} + \varepsilon R \right) \frac{\lambda_e I_1(bR) + \lambda_{ai} I_0(br_c)}{\lambda_{ai} b R I_1(bR)} \alpha(r_c) + (T_{ec} - T(r)) \alpha(r_c) \right] \tag{14} \end{aligned}$$

In the non-conducting zone the solution is:

$$\begin{aligned}
 T(r) - T(R) &= \frac{W}{2\pi\lambda} \ln \frac{R}{r} + \left(\frac{W}{2\pi\lambda} + \varepsilon R \right) \frac{\lambda_e [I_0(bR) - I_0(br)]}{\lambda_{ai} b R I_1(bR)} \\
 &\quad - \frac{W}{2\pi\lambda} \ln \frac{R}{r_c} \alpha(r_c) - \left(\frac{W}{2\pi\lambda} + \varepsilon R \right) \frac{\lambda_e I_0(bR) + \lambda_{ai} I_0(br_c)}{\lambda_{ai} b R I_1(bR)} \alpha(r_c) \\
 &\quad + (T_{ec} - T(R)) \alpha(r_c) T_e(r) - T(R) \\
 &= \frac{W}{2\pi\lambda} \ln \frac{R}{r} + \left(\frac{W}{2\pi\lambda} + \varepsilon R \right) \frac{\lambda_e I_0(bR) + \lambda_{ai} I_0(br)}{\lambda_{ai} b R I_1(bR)} \\
 &\quad - \frac{W}{2\pi\lambda} \ln \frac{R}{r_c} \beta(r) - \left(\frac{W}{2\pi\lambda} + \varepsilon R \right) \frac{\lambda_e I_0(bR) + \lambda_{ai} I_0(br_c)}{\lambda_{ai} b R I_1(bR)} \beta(r) \\
 &\quad + (T_{ec} - T(R)) \beta(r). \tag{15}
 \end{aligned}$$

where

$$\beta(r) = \frac{\lambda_e \Phi(R) + \lambda_{ai} \Phi(r)}{\lambda_e \Phi(R) + \lambda_{ai} \Phi(r_c)}; \tag{16}$$

$$\alpha(r) = \lambda_e \frac{\Phi(R) - \Phi(r)}{\lambda_e \Phi(R) + \lambda_{ai} \Phi(r_c)} \tag{17}$$

$$a^2 = \left. \frac{3 k \delta n_e \nu}{2 \lambda_{ai}} \right|_{0 < r < r_c} \tag{18}$$

$$b^2 = \left. \frac{3}{2} k \delta n_e \nu \left(\frac{1}{\lambda_{ai}} + \frac{1}{\lambda_e} \right) \right|_{r_c < r < R}; \tag{19}$$

and

$$\left. \frac{d\alpha}{dr} \right|_{r=R} = \left. \frac{d\beta}{dr} \right|_{r=R} = 0 \tag{20}$$

It is necessary to mention that solutions, Eqs. 14–15, were obtained as a result of solving the complete system, Eqs. 7–9, as opposed to the solution obtained by solving a simplified system of equations [1].

Equations 14–15 enable us to determine two unknowns $T_c \equiv T_c(T_{ec})$ and $T_0 \equiv T_0(T_{ec})$ in Eq. 6. Thus,

$$\begin{aligned}
 T_c \equiv T(0) &= T_{ec} - \frac{1}{I_0(ar_c)} \left\{ [T_{ec} - T(R)] [1 - \alpha(r_c)] - \frac{W}{2\pi\lambda} \ln \frac{R}{r_c} [1 - \alpha(r_c)] \right. \\
 &\quad - \left(\frac{W}{2\pi\lambda} + \varepsilon R \right) \frac{\lambda_e I_0(bR)}{\lambda_{ai} b R I_1(bR)} [1 - \alpha(r_c)] \\
 &\quad \left. + \left(\frac{W}{2\pi\lambda} + \varepsilon R \right) \frac{I_0(br_c)}{\lambda_{ai} b R I_1(bR)} [\lambda_e + \lambda_{ai} \alpha(r_c)] \right\} \tag{21}
 \end{aligned}$$

$$\begin{aligned}
 T_0 \equiv T(r_c) = T(R) + \frac{W}{2\pi\lambda} \ln \frac{R}{r_c} [1 - \alpha(r_c)] + \left(\frac{W}{2\pi\lambda} + \varepsilon R \right) \frac{\lambda_e I_0(bR)}{\lambda_{ai} b R I_1(bR)} \\
 \times [1 - \alpha(r_c)] - \left(\frac{W}{2\pi\lambda} + \varepsilon R \right) \frac{I_0(br_c)}{\lambda_{ai} b R I_1(bR)} [\lambda_e + \lambda_{ai} \alpha(r_c)] \\
 + [T_{ec} - T(R)] \alpha(r_c)
 \end{aligned} \tag{22}$$

Equations 6, 21, and 22 represent a transcendental system of equations used to find the exact value of the plasma temperature on the channel axis $T_e(0) \equiv T_{ec} \approx T_{e0} \equiv T_e(r_c)$ as a function of radius r_c of the current conducting area. Although Eqs. 21 and 22 are complicated at first glance, their implementation in practice is not difficult.

Having obtained T_{ec} and r_c , it becomes easy to obtain the remaining values, such as the gas temperature on the axis and boundary of the channel and the jump of the electronic temperature near the wall at $r = R$. Although a complete solution of the above system could be obtained with numerical methods for practical cases, using the Taylor and asymptotic behavior of functions $I_{0,1}(x)$, $K_{0,1}(x)$, it is easy to estimate the temperature values for small and large values of the argument, respectively. Therefore, in Eq. 8, by setting set $r = R$, we will obtain the following equations:

$$\begin{aligned}
 T_e(r) - T(R) = \left(\frac{W}{2\pi\lambda} + \varepsilon R \right) \frac{I_0(bR)\lambda}{b R I_1(bR)\lambda_{ai}} - \frac{W}{2\pi\lambda} \ln \frac{R}{r_c} \beta(R) - \left(\frac{W}{2\pi\lambda} + \varepsilon R \right) \\
 \times \frac{\lambda_e I_0(bR) + \lambda_{ai} I_0(br_c)}{\lambda_{ai} b R I_1(bR)} \beta(R) + [T_{ec} - T(R)] \beta(R),
 \end{aligned} \tag{23}$$

which is similar to the formula,

$$T_e(r) - T(R) = \left(\frac{W}{2\pi\lambda} + \varepsilon R \right) \frac{\lambda [K_0(br_c)I_0(bR) - I_0(br_c)K_0(bR)]}{\lambda_{ai} b R I_1(bR)\Phi(r_c)} \tag{24}$$

obtained using the simplified model [1].

Equation 23 allows the determination of the difference between the temperatures of the electron gas and the atom-ionic gas near the wall of the discharge limiting tube, as a function of the tube radius and the parameters of discharge.

3 Results

The results of the calculation of the electronic and gas temperatures (T_e and T) as functions of the radius are shown in Figs. 2, 3, 4. The experimental data are taken from Ref. [9]. The calculations are performed for argon plasma at atmospheric pressure and current $I = 30$ A and for different wall temperature values T_w (600 K, 2,600 K, 4,000 K).

It's necessary to note that the temperature of the wall surface could be higher than the melting temperature of the wall material. The authors of Ref. [9] found that after long-term operation, the interior surface of the channel appears to be covered with a dark layer of width no more than 0.1 mm. Most likely, this dark film is formed as a

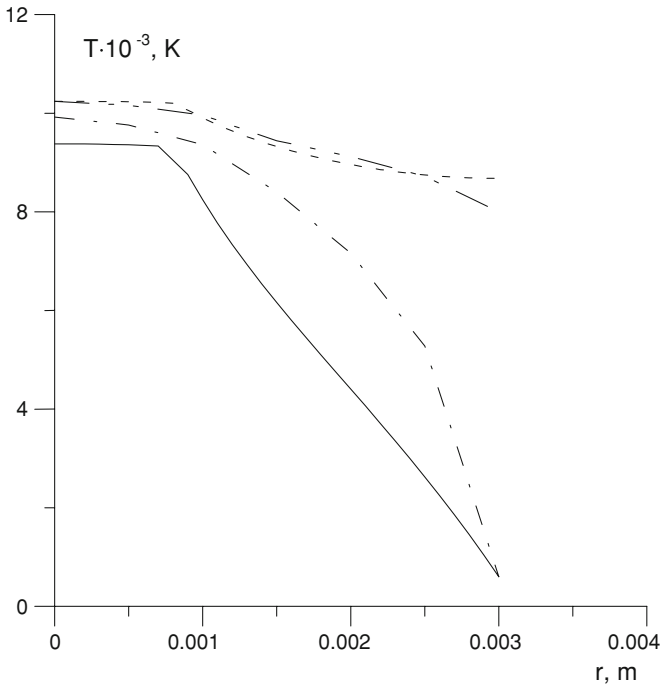


Fig. 2 Distribution electronic T_e and gas T temperatures on radius of a column of an arc for temperature of a wall $T_w = 600$ K: ——— calculation for atomic–ionic temperature; - - - - calculation for electronic temperature; — - data of Asinovskii and Pakhomov [9] for atomic–ionic temperature; — · - data of Asinovskii and Pakhomov [9] for electronic temperature

result of condensation of carbon vapors onto the cold wall. As stated in [9], this layer has a large thermal resistance, the consequence of that being that the temperature of the wall at the plasma boundary can rise to 4,000 K. The values λ_e , λ_{ai} , n_e , δ , and ν are taken from [7, 10–12].

The results published in Ref. [9] are represented in the foregoing figures. The calculations involved the following procedure: The channel radius r_c , the gas temperature on the boundary of the conducting area T_0 , and that on the axis T_c were determined by solving the transcendental system of Eqs. 6, 21, and 22 at the given value of channel temperature, T_{ec} . Then, the calculation of gas and electronic temperatures throughout the entire volume of discharge (both inside and outside the current-conducting area) was performed using Eqs. 14–15.

4 Discussion

As we can see from the forgoing figures, the best agreement of the results is observed for electronic temperature T_e . As for the atomic–ionic temperature of heavy particles, the best agreement occurs when the temperature of the wall $T(R)$ is sufficiently

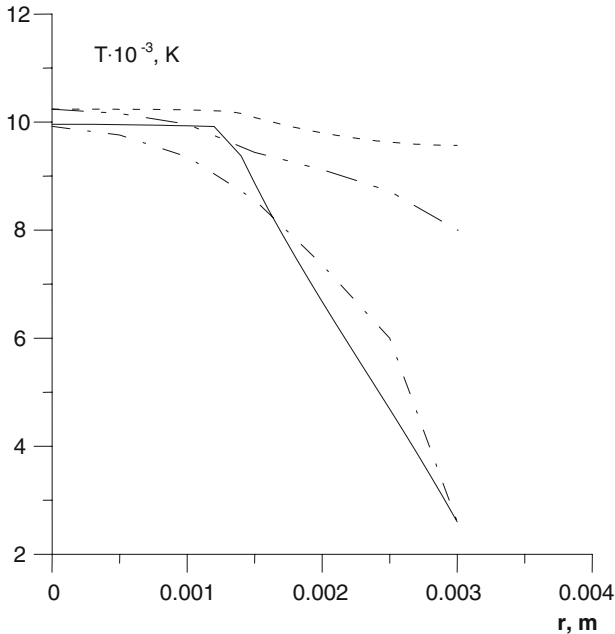


Fig. 3 Distribution electronic T_e and gas T temperatures on radius of a column of an arc for temperature of a wall $T_w = 2,600$ K: ——— calculation for atomic–ionic temperature; - - - - calculation for electronic temperature; — - data of Asinovskii and Pakhomov [9] for atomic–ionic temperature; — · - data of Asinovskii and Pakhomov [9] for electronic temperature

large. This may be explained by the fact that the existence of temperature and particle concentration gradients at the radial section of the channel cause the formation of heat and mass flows at relatively low wall temperatures. The electrons and ions move toward the wall while the atoms and molecules move toward the axis. In addition, the concentration of charged particles decreases in the wall zone, and the electrons cannot transfer all the energy obtained from the electric field to heavy particles.

Moreover, the figures show that the radius of the conductive channel is increased with increasing wall temperature. This is explained by the decreasing temperature and concentration gradients as well as by the increase of the heating efficiency of heavy particles through scattering with electrons.

The calculations performed with Eqs. 21 and 22 show that at fixed axial temperature T_c , the radius of the conducting zone is larger than the one calculated using the formula of the classic equilibrium model of a cooled arc. From a physical standpoint, this means that the energy dissipation mechanism in the two-temperature model is less effective because of the thermal equilibrium discharge. Hence, in order to satisfy the requirements of the energy balance equations, it is necessary that the heat flow density from the central zone of the heat generation (at $r < r_c$) $J \sim W/(2\pi r_c)$ in the non-equilibrium case is less than the value calculated using the

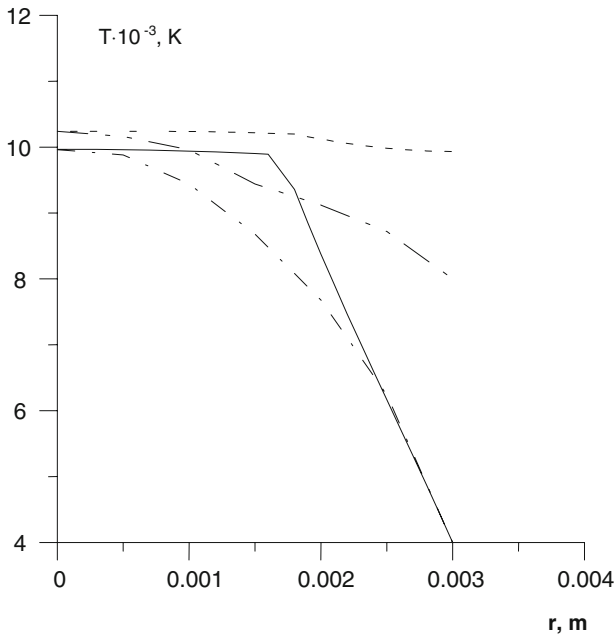


Fig. 4 Distribution electronic T_e and gas T temperatures on radius of a column of an arc for temperature of a wall $T_w = 4,000$ K: ——— calculation for atomic–ionic temperature; - - - - - calculation for electronic temperature; — - - data of Asinovskii and Pakhomov [9] for atomic–ionic temperature; - - - data of Asinovskii and Pakhomov [9] for electronic temperature

formula for the one-temperature model [1], so that the condition $r_c^{T \neq T_e} > r_c^{T = T_e}$ will be satisfied.

Finally, the results published in [13] and [14] sufficiently confirm all of the basic results and the pattern of heat exchange in the dual-temperature arc discharge in a long cylinder tube obtained in this study.

5 Conclusion

The proposed method offers the possibility to obtain the distribution of gas and electron temperatures as functions of the radial coordinate in the channel of an arc plasmatron with rather high precision for given discharge parameters (current intensity, power, etc). For a valid quantitative comparison between the theory and experiments, more detailed information about the composition of the non-equilibrium plasma, its thermo-physical parameters, and coefficients is required. The formulas obtained in this article describe the distribution of temperature fields in an axi-symmetric arc discharge, and may be used for parameter estimation rather than the interpretation of complicated physical processes.

References

1. A.V. Gerasimov, A.P. Kirpichnikov, *Therm. Sci.* **2**, 101 (2003)
2. Yu.P. Raizer, *Basis of a Modern Physics of Gas-Discharge Processes* (Nauka, Moscow, 1980), pp. 165–172
3. Yu.P. Raizer, *Physics of Gas Discharge* (Nauka, Moscow, 1987), pp. 443–444
4. A. Engel, M. Steenbeck, *Electrische gasentladungen ihre physik und technic. Zweiter Band. Entladungseigenschaften. Technische anwendungen* (Verlag von Julius Springer, Berlin, 1934)
5. H.W. Emmons, *Phys. Fluids* **10**, 1125 (1967)
6. R.S. Devoto, *Phys. Fluids* **9**, 1230 (1966)
7. S.V. Dresvin (ed.), *Physics and Technique of Low-Temperature Plasma* (Atomizdat, Moscow, 1972), pp. 279–281
8. K.J. Clark, F.P. Incropera, *AIAA Paper* **71-593**, 15 (1971)
9. E.I. Asinovskii, E.P. Pakhomov, *High. Temp.* **6**, 333 (1968)
10. R.S. Devoto, *Phys. Fluids* **16**, 616 (1973)
11. V.L. Ginzburg, *Electromagnetic Wave Propagation in Plasma* (Nauka, Moscow, 1967), pp. 75–92
12. M.F. Gukov (ed.), *Properties of the Low-Temperature Plasma and Methods of its Diagnostics* (Nauka, Novosibirsk, 1977), pp. 26–29
13. L.S. Polak (ed.), *Chemical Reactions in Low-Temperature Plasma* (Institute of petrochemical synthesis, Moscow, 1977), pp. 83–103
14. E.I. Asinovskii, E.P. Pakhomov, Y.M. Yartsev, *High Temp.* **16**, 28 (1978)